# Epithelial Hexokinase 2 expression is a marker for intestinal inflammation

Saskia Weber-Stiehl[1*], Jan Taubenheim[2*], Lea Järke[1*], Christoph Röcken[3], Stefan Schreiber[4], Konrad Aden[1,4], Christoph Kaleta[2], Philip Rosenstiel[1], Felix Sommer[1]

[1] Institute of Clinical Molecular Biology, University of Kiel, Rosalind-Franklin-Straße 12, 24105 Kiel, Germany

[2] Institute of Experimental Medicine, University of Kiel, Michaelisstr. 5, 24105 Kiel, Germany

[3] Department of Pathology, University Hospital Schleswig-Holstein, Campus Kiel, Arnold-Heller-Straße 3/House U33, 24105 Kiel, Germany

[4] Department of Internal Medicine I, University Hospital Schleswig-Holstein, Campus Kiel, 24105 Kiel, Germany

[*] These authors contributed equally with shared first authorship.

**Correspondence:** Felix Sommer, Institute of Clinical Molecular Biology (IKMB), Christian-Albrechts-University (CAU) Kiel, Rosalind-Franklin-Str. 12, Kiel D-24105, Germany; tel: +49(0) 431/500-15146; email: f.sommer@ikmb.uni-kiel.de

**Keywords:** inflammation / hexokinase / HK2 / human biopsies

**Abstract**

**Background:** Inflammation is characterized by a metabolic switch promoting glycolysis and lactate production. Hexokinases (HK) catalyze the first reaction of glycolysis and inhibition of epithelial HK2 protected from colitis in mice. HK2 expression has been described as elevated in patients with intestinal inflammation, however there is conflicting data from few cohorts especially with severely inflamed individuals, thus systematic studies linking disease activity with HK2 levels are needed.

**Methods:** We therefore examined the relationship between HK2 expression and inflammation severity using transcriptome data derived from the mucosa of thoroughly phenotyped patients suffering from intestinal inflammation. The mucosa undergoes a cellular remodeling during inflammation due to an infiltration of HK2-negative immune cells and a loss of the apical epithelium – the main site of HK2 expression.

**Results:** Normalizing for the epithelial loss clearly identified epithelial HK2 expression as gradually increasing with disease activity and remaining elevated at high inflammation scores. We then performed immunofluorescence analyses on colonic biopsies of unrelated patients with intestinal inflammation and confirmed the RNA-based findings on protein level. HK2 protein expression was mostly restricted to brush border enterocytes and these cells along with HK2 levels vanished with increasing disease severity.

**Conclusions:** Our findings clearly define dysregulated epithelial HK2 expression as an indicator of disease activity in intestinal inflammation and suggest targeted HK2-inhibition as a potential therapeutic avenue.

## Introduction

Prevalence of inflammatory bowel disease (IBD) is rising globally causing severe health issues and drastically reducing quality of life. These diseases are multifactorial with complex interactions of multiple genetic and environmental factors[1]. Despite decades of intense research, the exact etiology of IBD remains mostly unknown limiting treatment options[2]. In recent years it became evident that ongoing inflammation is characterized by changes in metabolic activity, in particular glucose metabolism[3–5]. Hexokinases (HK) catalyze the first and irreversible step of glycolysis – the phosphorylation of glucose to glucose-6-phosphate – and are therefore crucial for glucose metabolism and maintenance of homeostatic body functions. In mammals, five HK isoenzymes have been identified: HK1, HK2, HK3, GCK (Glucokinase) and HKDC1 (HK domain containing 1). Each of these HK isoenzymes display specific tissue expression patterns and glucose affinities. HK2 is of particular interest as it is the most abundant HK member within the intestine, exerts high HK activity, responds to various internal as well as external stimuli and shows elevated levels during inflammation[6]. Recently, we further revealed an upregulated expression of HK2 specifically in inflamed compared to non-inflamed tissue of the same patient, irrespective of the type of intestinal inflammation and demonstrated that ablation of HK2 in intestinal epithelial cells (IEC) protects from acute intestinal inflammation, suppresses cell death and alters mitochondrial function[6]. These findings placed HK2 as a molecular target to treat intestinal inflammation. However, when expanding our research about the role of HK2 in intestinal inflammation, we encountered transcriptome datasets with contradictory findings of either an unaltered HK2 expression or even downregulation, especially in severely inflamed patients undergoing bowel resection[7]. We therefore aimed to investigate the cause of this apparent contradiction with the goal to clarify the relation between HK2 expression and intestinal inflammation. Here, we show that with increasing inflammation severity the intestinal mucosa is gradually remodeled, which comprises a partial loss of the apical epithelium – the primary source of HK2 expression – and a simultaneous infiltration of immune cells. Normalizing for this cellular remodeling clearly demonstrates a gradual upregulation of HK2 expression with severity of intestinal inflammation.

## Results

### Epithelial HK2 expression increases with high inflammation scores

To determine a possible correlation of HK2 expression and disease activity, we analyzed RNA sequencing (RNA-seq) data derived from intestinal biopsies of patients suffering from IBD of two independent clinical studies[8,9], for which accompanying disease activity scores for each sample were available. This analysis revealed that HK2 expression initially increased gradually reaching peak expression at mid disease activity (inflammation score ~ 0.4) and then declined with high inflammation scores (Figure 1A). As within the intestine HK2 is mainly expressed by epithelial cells of the apical mucosa (Figure S1), we hypothesized that with very high levels of inflammation these apical epithelial cells and therefore also the main site of HK2 expression might be lost due to shedding and apoptosis or transdifferentiation resulting in decreased HK2 expression levels in bulk RNA-seq data. To investigate this hypothesis, we assessed the expression levels of three different epithelial marker genes, namely E-cadherin (*ECAD*), epithelial cell adhesion molecule (*EPCAM*) and Villin1 (*VIL1*). Supporting our hypothesis, the expression levels of these epithelial markers were all declining with increasing inflammation severity (Figure 1B-D), which indicates progressive epithelial damage caused by the inflammation. To account for this epithelial loss, we then normalized the expression of HK2 to that of these epithelial markers, thereby yielding an epithelial HK2 expression. Importantly, epithelial HK2 expression gradually increased in correlation to disease activity and then remained elevated at high inflammation scores (Figure 1E). To test whether the observed expression changes were unique to the combined clinical cohorts, we also performed these analyses separately for each clinical cohort (Figure S2). Importantly, we observed for both clinical cohorts the same changes in *HK2*, *ECAD*, *EPCAM*, *ECAD* and epithelial HK2 expression. We also tested for potential differences between the two main types of IBD, Crohn´s disease (CD) and ulcerative colitis (UC) and found similar responses both for CD and UC (Figure S3). Finally, correlation of HK2 expression with disease severity was confirmed using linear regression models (Figure S4 and Table S1).

### Immune cell infiltration during intestinal inflammation

99 Another source for cellular remodeling during inflammation is tissue infiltration by immune
100 cells. Using the bulk RNA-seq data we also investigated the proportions of various immune
101 cell types in relation to disease severity. First, we performed a candidate gene-based analysis
102 and chose several immune marker genes to assess infiltration of T cells, T helper 1 (Th1) cells,
103 T helper 2 (Th2) cells, B cells, basophils, neutrophils, eosinophils, and macrophages (Figure
104 2A). In contrast to *HK2* and the epithelial marker genes, the expression of these individual
105 immune cell genes increased with the inflammation score. However, slight alterations in the
106 expression patterns could be observed, mostly depending on the immune cell type.
107 Expression of the T cell marker genes *TRAC*, *CD3D* and *CD3E,* the B cell marker gene *CD19,* the
108 eosinophil marker gene *CCR2*, the neutrophil marker genes *CD14* and *CXCR4* as well as the
109 basophil marker genes *ITGA2B* and *ITGA4* all gradually increased in a linear fashion with the
110 inflammation score (Figure 2). In contrast, the marker genes for Th2 (*IL4*, *IL5*, *IL13*), Th1 (*IFNG*,
111 *IL12*) cells and macrophages (*ITGAM*, *IL1B*) all only displayed biphasic expression patterns
112 with a first phase characterized by slight increases in expression until an inflammation score
113 of approximately 0.5 and a second phase at higher disease severity characterized by larger
114 changes in their expression. The greatest expression changes were detected for the
115 macrophage marker genes *ITGAM* and *IL1B* suggesting the greatest relative increase of these
116 cells with increasing disease activity. Normalizing *HK2* expression to the candidate immune
117 cell genes revealed gradual declines with increasing inflammation scores for all tested
118 immune cell types indicating that the immune cell infiltration leads to more cells present in
119 the mucosa, which do not or only express very little *HK2* (Figure 2B).

120 Next, we moved from the candidate gene-based to a systematic cellular deconvolution of the
121 bulk RNA-seq data using MuSiC[10]. This program uses a reference single cell data set and cell
122 type-specific expression profiles to derive the abundance of the individual cell types from bulk
123 RNA-seq data. We restricted this analysis to the eight most abundant cell types. The
124 proportion of epithelial cells gradually declined with increasing inflammation scores whereas
125 the proportion of macrophages, B cells and regulatory T cells increased (Figure 3A). The
126 proportion of mast, cytotoxic T cells and dendritic cells remained mostly unchanged.
127 Therefore, this data indicates a massive gradual cellular remodeling of the intestinal mucosa
128 during inflammation and the findings of the systematic cellular deconvolution supported
129 those of the candidate gene-based analyses. Furthermore, the drastic decrease in the

130 proportion of epithelial cells with increasing inflammation scores demonstrates again that the
131 main source of *HK2* expression is lost during the disease course. This is therefore also
132 reflected by the outcome that after accounting for the abundance of epithelial cells the
133 normalized epithelial *HK2* expression gradually increased with disease severity (Figure 3B).

134

135 **Apical HK2 expression in mature enterocytes correlates with inflammation severity**

136 To validate the transcriptome data and to elucidate the biogeography of the changes in tissue
137 architecture in relation to HK2 expression, we performed immunostainings on colonic
138 biopsies of an independent set of UC patients that had been thoroughly scored for histological
139 disease severity (Nancy score). HK2 protein levels increased non-significantly in mildly
140 inflamed (score 1) compared to non-inflamed specimen (score 0) and remained unaltered at
141 medium or strong inflammation (scores 2 and 4) (Figure 4A,C). In contrast, protein levels of
142 the epithelial marker E-cadherin (ECAD) were unchanged in mild (score 1) but non-
143 significantly reduced at medium or strong inflammation (scores 2 and 4) compared to non-
144 inflamed control samples (Figure 4A,C). Notably, structural epithelial damage of inflamed
145 biopsies was detectable with increasing inflammatory scores (Figure 4C) with loss of epithelial
146 cells and an infiltration of other cells, probably immune cells, into the inflamed mucosa. In
147 addition, many epithelial cells that were not shed but still present at the inflamed site had
148 reduced ECAD expression, which could indicate transdifferention of these inflamed apical
149 enterocytes. Normalizing the HK2 protein levels to those of ECAD revealed that epithelial HK2
150 protein levels (Figure 4B) significantly increased with inflammation regardless of disease
151 severity (scores 1-4). This epithelial HK2 protein expression in inflamed intestinal mucosal
152 biopsies mirrored and confirmed the transcript patterns of the RNA sequencing analysis.

153 Furthermore, we used recently-published data from single cell RNA sequencing of mucosal
154 biopsies from IBD patients[11] to investigate the *HK2* expression on a cellular level in relation to
155 intestinal inflammation. This analysis of single cell RNA sequencing data confirmed our
156 findings from the bulk RNA sequencing and immunofluorescence, as *HK2* was mainly
157 expressed by mature enterocytes and then followed by goblet cells and immature
158 enterocytes (Figure 5A,B). Next, we checked for *HK2* expression pattern in enterocytes at
159 different inflammatory stages (healthy vs. inflamed vs. non-inflamed) and found that the
160 lowest *HK2* expression can be observed in healthy controls, while cells from inflamed samples

161 showed an increased HK2 expression (Figure 5C). Non-inflamed samples had intermediate
162 *HK2* expression levels (Figure 5C), which indicates that HK2 expression is dysregulated in
163 enterocytes of IBD patients also in the absence of an overt inflammation. This pattern of *HK2*
164 expression was also present although less predominant in immature enterocytes and goblet
165 cells. Finally, we looked into the number of these three cell types that are detected in the
166 three health states and found that mature and immature enterocytes are lost during
167 inflammation, while incomplete recovery can be observed in non-inflamed tissue of IBD
168 patients (Figure 5D). Altogether, the single cell data therefore supports a cellular
169 reprogramming during inflammation with loss of mature enterocytes (the main cell type of
170 the apical epithelium) and a dysregulated *HK2* expression in inflamed apical epithelial cells.

171 In summary, both the RNA and protein data clearly demonstrate that epithelial HK2 was
172 overexpressed during intestinal inflammation, which highlights HK2 as an indicator of active
173 disease. Building upon previous findings from murine models that inhibition of HK2
174 expression either genetically or via the microbial metabolite butyrate protect from
175 experimental colitis[6], these new data now show that indeed HK2 expression is dysregulated
176 in the mucosa of patients with active inflammation and therefore suggest that targeting HK2
177 may represent a promising approach to suppress intestinal inflammation in humans.

178 **Discussion**

179 There is a growing need for valid disease biomarkers and molecular targets for intestinal
180 inflammation as prevalence is increasing and despite significant efforts the cause of these
181 diseases remains unknown. In a recent study, HK2 was identified as upregulated under
182 inflammatory conditions in mice and humans irrespective of disease subtype (CD, UC or non-
183 IBD colitis) and suppressing HK2 expression even protected from experimental colitis[6] placing
184 HK2 as a potential disease marker. However, we found other transcriptome datasets
185 generated from severely inflamed patients in which HK2 expression was unaltered or even
186 reduced[7]. Here, we therefore thoroughly investigated the relationship between HK2
187 expression and disease severity by analyzing transcriptome data derived from intestinal
188 biopsies of patients with intestinal inflammation for which corresponding data on disease
189 severity (HBI, Mayo score, Nancy score) were available. In addition, we performed cellular
190 deconvolution analyses of the RNA sequencing data to infer the changes in cell proportions
191 during inflammation. Finally, we used immunofluorescence staining to clarify the changes in
192 HK2 protein biogeography in the mucosa during inflammation. Using these approaches, we
193 demonstrated that raw HK2 RNA and protein expression at first gradually increased with the
194 inflammation scores, yet after reaching a critical inflammation score HK2 expression declined
195 again at very severe inflammation. These findings integrate the seemingly conflicting data
196 from previous studies[7,12–14] by linking HK2 expression to disease severity. We further were
197 able to demonstrate that loss of HK2 expression at high inflammation levels was dependent
198 on the disruption of brush border enterocytes as both the expression of epithelial marker
199 genes were decreasing with the inflammation score and immunofluorescence analyses clearly
200 pointed to a destruction of the apical epithelium – the main site of HK2 expression[15,16]. These
201 findings are in line with clinical practice, in which epithelial damage is a key criterion to classify
202 an increasing inflammatory state during IBD[17], for example with epithelial erosion being a
203 feature of histological inflammation in the Nancy score. By analyzing single cell RNA
204 sequencing data derived from an independent set of UC patients, we confirmed that in the
205 gut epithelial cells are the main source of *HK2* expression, both in terms of per cell expression
206 as well as the number of cells contributing to overall expression (Figure 5). These cells are
207 consequently lost due to increasing inflammation in the single cell data set, which would
208 explain the decrease of *HK2* expression at high levels of inflammation[11]. Finally, we were able

209 to deconstruct the simultaneous epithelial erosion and immune cell infiltration into the
210 submucosa during intestinal inflammation from the RNA sequencing data. Based on the
211 overall abundance and their induction (fold change) during inflammation, infiltrating
212 macrophages seemed most relevant, but also other cell types such as B cells increased in
213 proportion. Especially the expansion of macrophages could be important and contributing to
214 the loss of epithelial cells and therefore HK2 expression during inflammation as IL-1β
215 interferes with the tight junction complexes between IECs[11–13] and thereby increases
216 intestinal permeability[21]. Similar to epithelial erosion, immune cell infiltration is a classical
217 feature of inflammation and used in clinical practice to histologically evaluate disease
218 severity, in particular as a feature of the Nancy score[22]. In addition, transdifferentiation of
219 HK2-positive mature enterocytes into other cell types such as HK2-negative immature
220 enterocytes and stem cells[23,24] or maybe even into mesenchymal cells as during epithelial–
221 mesenchymal transition [25] could also contribute to a reduction of HK2 levels in the inflamed
222 mucosa. In summary, our findings imply that during the course of inflammation, changes in
223 the cellular composition of the mucosa, i.e. loss of brush border epithelial cells expressing
224 high levels of HK2 and a corresponding massive recruitment of immune cells expressing little
225 to no HK2 to the site of inflammation, affect the overall bulk HK2 expression leading to an
226 overall reduction despite higher expression levels in fewer and fewer HK2-positive cells
227 (Figure 6). Overall, we want to highlight the importance of taking into consideration the
228 biogeography and changes in cell type expression ratios, when trying to identify disease
229 biomarkers, especially regarding complex diseases such as intestinal inflammation involving
230 various internal and external factors. Most previous studies used bulk expression data in the
231 search for disease biomarkers or therapeutic targets and therefore may have missed other
232 locally restricted but disease relevant genes like *HK2*. In our analyses HK2 expression was only
233 significantly associated with disease severity after considering epithelial cell abundance
234 (Figure 1E and Figure 3B) and we speculate that this pattern will also hold true for other genes
235 with an apical or otherwise restricted expression. For example, other hexokinases (HK1,
236 HKDC1), proteins responsible for the uptake of dietary nutrients (e.g. SGLT1, SLC15A1) or
237 those contributing to the intestinal epithelial barrier (e.g. CLDN15, ZO-1) also show a
238 predominant or even restricted apical expression and therefore possibly have not yet been
239 identified as disease biomarker during severe intestinal inflammation due to the loss of their
240 primary expression site. Notably, epithelial remodeling not only includes the partial loss of

241 apical enterocytes and infiltration of lymphocytes, but also includes hyperregeneration,
242 metaplasia and a loss of goblet cells. The advent of single cell technologies such as single cell
243 RNA sequencing promise to pave the way for more refined analyses that will enable the
244 discovery of more suitable disease markers and to enhance our understanding of the
245 molecular and cellular mechanisms during disease progression.

246

247 **Conclusions**

248 HK2 has not yet been described as IBD risk gene, most probably due to its site-restricted
249 expression, but here we were able to show an association of HK2 and epithelial status during
250 intestinal inflammation. Therefore, epithelial HK2 expression correlates with disease severity
251 making it a useful indicator of intestinal inflammation and highlighting the therapeutic
252 potential of targeting HK2. However ultimately, clinical studies are required to indeed
253 demonstrate the feasibility and efficacy of a HK2-targeted intervention in IBD patients.

254 **Materials and methods**

255 **Human studies**

256 We used mucosal transcriptomic data and fixed intestinal specimen of two independent large
257 longitudinal clinical studies, namely the EMED[9] (191 samples) and FUTURE[8] (86 samples)
258 cohorts (trial IDs: EudraCT number 2016-000205-36 and ClinicalTrials.gov NCT02694588), for
259 which accompanying disease activity scores (Harvey-Bradshaw Index (HBI)/Mayo Score) were
260 available. The HBI[26] is used to quantify disease activity in patients suffering from Crohn's
261 disease (CD), one of the two IBD subtypes. Here, variables such as general well-being,
262 abdominal pain and abdominal mass with each having scores of 0-3, as well as the number of
263 liquid stools per day (1 point per stool) and other complications (1 point per complication)
264 yield the "open-ended" total score (Table S2). The Mayo score is used for ulcerative colitis
265 (UC), the other clinical IBD subtype. This scoring system accounts for general well-being, rectal
266 bleeding, endoscopic results and stool frequency with scores of 0-3 per category for an overall
267 score ranging from 0 to 12 (Table S2). To facilitate a direct comparison of both scores despite
268 them being "open-ended" and "discrete", we calculated a general inflammation score by
269 setting the highest score in the dataset for each HBI and Mayo score to 1 and scaled the score
270 of each patient accordingly (see Table S2).

271

272 **Transcriptome data analysis**

273 RNA sequencing data derived from mucosal biopsies of patients with various grades of
274 intestinal inflammation were retrieved from two previously published IBD cohorts[8,9]. Read
275 counts were transformed to Transcripts Per Million (TPM) values to normalize for differential
276 sequencing depths among samples. TPM data were then plotted per sample against the
277 inflammation score using R (version 4.2.2) and ggplot2 (3.4.3). Trendlines were calculated
278 including all data points and using the distance to the actual location as a weight to enable a
279 robust calculation and avoiding overfitting especially in areas of scarce sampling. To test for
280 an association of gene expression to changes in the inflammation score we used variance-
281 stabilization transformation of raw read counts and fitted linear mixed models with following
282 form: vst(geneExpression) ~ Age + Gender + Diagnosis + InflammationScore. Statistical
283 analyses were performed using R (version 4.2.2[27] with the following packages: lm4 (version

284 1.1-29)[28], lmerTest (version 3.1-3)[29], car (version 3.0-13)[30], ggplot2 (version 3.3.6)[31] and
285 DESeq2 (version 1.38.3)[32].
286
287 **Cellular deconvolution**
288 We deconvoluted the bulk RNA data using the MuSiC package (version 1.0.0)[10] with default
289 values. As reference, we used a single cell data set from UC patients described in a study by
290 Smillie et. al.[11]. The original single cell data set was split in "epithelial", "immunogenic" and
291 "stromal" subsets, which we rejoined in our analysis. Due to limited resolution in
292 deconvolution approaches and to reduce cell diversity, we pooled ontogenetically closely
293 related cell types (Table S3). We restricted the analysis to the eight most abundant cell types.
294
295 **Single cell RNA sequencing**
296 Single cell data was obtained from the Single Cell Portal (accession SCP259) initially described
297 by Smillie and colleagues[11]. The different cell populations were rejoined and general quality
298 controls were performed. In short, we filtered cells with read counts below 1000 (low quality).
299 Further, we removed cells with less than 200 or with more than 2720 (two-fold of the
300 standard deviation of expressed genes across all cells) differently expressed genes to account
301 for spurious sequencing depth and removal of duplicates. All cells with a mitochondrial RNA
302 content above 5% were also removed. For plotting, gene expression values where log-
303 transformed. Plotting and quality filtering was performed in R (version 4.2.2) using ggplot2
304 (version 3.4.3) and Seurat (version 4.4.0)[33].
305
306 **Immunofluorescence**
307 5 µm sections of paraffin-embedded colonic biopsies were deparaffinized with Xylol
308 substitute (Roth), incubated in citrate buffer for 3 minutes and subsequently blocked in 5 %
309 BSA-PBS and 0,2 % TritonX for 30 minutes. Primary anti-E-cadherin (1:400 in 1 % BSA, #3195,
310 Cell Signaling Technology) and anti-Hexokinase 2 (1:500 in 1% BSA, Cat# NBP2-02272, Novus
311 Biologicals, Colorado, US) antibodies were incubated over-night. Sections were washed,
312 incubated with secondary antibodies (Alexa Fluor 488 goat anti mouse, Invitrogen, A32731
313 and Alexa Fluor 555 goat anti rabbit, Invitrogen, A21430) for 45 minutes at room
314 temperature. DAPI (1:40000 in PBS, D9542, Sigma Aldrich, St. Louis, US) was used for DNA
315 counterstaining. Slides were mounted using antifade mounting media (DAKO, Hovedstaden,

316 Denmark). The quantitative analysis was performed using fluorescence microscopy for
317 stained samples using the imager Z1 microscope (ZEISS, Jena, Germany) and ZEN software
318 (version 3.0). Images were taken by a digital camera system (AxioCam HrC/HrM, Zeiss, Jena,
319 Germany) and ApoTome (ZEISS, Jena, Germany). Fluorescence signal intensity was measured
320 using Fiji/ImageJ software.
321
322 **Statistics**
323 General statistical analyses were performed using the GraphPad Prism 9 (GraphPad Software
324 Inc., La Jolla, USA). For pairwise comparisons the Mann-Whitney-U test was used whereas for
325 multiple comparisons one-way ANOVA with false discovery rate (FDR) correction were
326 performed. Data are shown as mean ± standard error of the mean (SEM). A p-value of ≤ 0.05
327 was considered as significant (*). A p-value of ≤ 0.01 was considered as strongly significant
328 (**) and p-value of ≤ 0.001 as highly significant (***). For longitudinal data, linear mixed effect
329 models were fitted with where gene expression was used as dependent variable, while
330 inflammation score and patient ID were fixed and random factors. The models were fitted
331 using lme4 (version 1.1-31) and statistical testing for coefficients was performed using
332 lmerTest (version 3.1-3). Model validity was tested against a null-model using log-likelihood
333 ratio tests and model assumption were evaluated by diagnostic plotting of model residuals,
334 data point influence strength and random factor fitting.
335

336 **References**


337 1. Kaplan, G. G. & Windsor, J. W. The four epidemiological stages in the global evolution of
338 inflammatory bowel disease. *Nat Rev Gastroenterol Hepatol* **18**, 56–66 (2021).
339 2. Kaplan, G. G. The global burden of IBD: from 2015 to 2025. *Nat Rev Gastroenterol*
340 *Hepatol* **12**, 720–727 (2015).
341 3. Rath, E. & Haller, D. Intestinal epithelial cell metabolism at the interface of microbial
342 dysbiosis and tissue injury. *Mucosal Immunology* **15**, 595–604 (2022).
343 4. Gaber, T., Strehl, C. & Buttgereit, F. Metabolic regulation of inflammation. *Nature*
344 *Reviews Rheumatology* **13**, 267–279 (2017).
345 5. Soto-Heredero, G., Gómez de las Heras, M. M., Gabandé-Rodríguez, E., Oller, J. &
346 Mittelbrunn, M. Glycolysis – a key player in the inflammatory response. *FEBS J* **287**,
347 3350–3369 (2020).
348 6. Hinrichsen, F. *et al.* Microbial regulation of hexokinase 2 links mitochondrial metabolism
349 and cell death in colitis. *Cell Metab* **33**, 2355-2366.e8 (2021).
350 7. Peters, L. A. *et al.* A functional genomics predictive network model identifies regulators of
351 inflammatory bowel disease. *Nat Genet* **49**, 1437–1449 (2017).
352 8. Schreiber, S. *et al.* Therapeutic Interleukin-6 Trans-signaling Inhibition by Olamkicept
353 (sgp130Fc) in Patients With Active Inflammatory Bowel Disease. *Gastroenterology* **160**,
354 2354-2366.e11 (2021).
355 9. Zeissig, S. *et al.* Vedolizumab is associated with changes in innate rather than adaptive
356 immunity in patients with inflammatory bowel disease. *Gut* **68**, 25–39 (2019).
357 10. Wang, X., Park, J., Susztak, K., Zhang, N. R. & Li, M. Bulk tissue cell type deconvolution
358 with multi-subject single-cell expression reference. *Nat Commun* **10**, 380 (2019).

359 11. Smillie, C. S. *et al.* Intra- and Inter-cellular Rewiring of the Human Colon during
360 Ulcerative Colitis. *Cell* **178**, 714-730.e22 (2019).
361 12. Marigorta, U. M. *et al.* Transcriptional risk scores link GWAS to eQTLs and predict
362 complications in Crohn's disease. *Nat Genet* **49**, 1517–1521 (2017).
363 13. Haberman, Y. *et al.* Pediatric Crohn disease patients exhibit specific ileal transcriptome
364 and microbiome signature. *J. Clin. Invest.* **124**, 3617–3633 (2014).
365 14. Quraishi, M. N. *et al.* A Pilot Integrative Analysis of Colonic Gene Expression, Gut
366 Microbiota, and Immune Infiltration in Primary Sclerosing Cholangitis-Inflammatory
367 Bowel Disease: Association of Disease With Bile Acid Pathways. *Journal of Crohn's and*
368 *Colitis* **14**, 935–947 (2020).
369 15. Sommer, F., Nookaew, I., Sommer, N., Fogelstrand, P. & Bäckhed, F. Site-specific
370 programming of the host epithelial transcriptome by the gut microbiota. *Genome Biol*
371 **16**, 62 (2015).
372 16. The Tabula Muris Consortium *et al.* Single-cell transcriptomics of 20 mouse organs
373 creates a Tabula Muris. *Nature* **562**, 367–372 (2018).
374 17. Guan, Q. A Comprehensive Review and Update on the Pathogenesis of Inflammatory
375 Bowel Disease. *Journal of Immunology Research* **2019**, 1–16 (2019).
376 18. Coccia, M. *et al.* IL-1β mediates chronic intestinal inflammation by promoting the
377 accumulation of IL-17A secreting innate lymphoid cells and CD4+ Th17 cells. *Journal of*
378 *Experimental Medicine* **209**, 1595–1609 (2012).
379 19. Chotikatum, S., Naim, H. Y. & El-Najjar, N. Inflammation induced ER stress affects
380 absorptive intestinal epithelial cells function and integrity. *International*
381 *Immunopharmacology* **55**, 336–344 (2018).

382 20. Lin, Y. *et al.* Non-hematopoietic STAT6 induces epithelial tight junction dysfunction and
383 promotes intestinal inflammation and tumorigenesis. *Mucosal Immunology* **12**, 1304–
384 1315 (2019).
385 21. He, L. *et al.* Gut Epithelial Vitamin D Receptor Regulates Microbiota-Dependent Mucosal
386 Inflammation by Suppressing Intestinal Epithelial Cell Apoptosis. *Endocrinology* **159**,
387 967–979 (2018).
388 22. Marchal-Bressenot, A. *et al.* Development and validation of the Nancy histological index
389 for UC. *Gut* **66**, 43–49 (2017).
390 23. Moor, A. E. *et al.* Spatial Reconstruction of Single Enterocytes Uncovers Broad Zonation
391 along the Intestinal Villus Axis. *Cell* **175**, 1156-1167.e15 (2018).
392 24. Wei, X. *et al.* Extensive jejunal injury is repaired by migration and transdifferentiation of
393 ileal enterocytes in zebrafish. *Cell Reports* **42**, 112660 (2023).
394 25. López-Novoa, J. M. & Nieto, M. A. Inflammation and EMT: an alliance towards organ
395 fibrosis and cancer progression. *EMBO Mol Med* **1**, 303–314 (2009).
396 26. Harvey, R. F. & Bradshaw, J. M. A Simple Index Of Crohn's-Disease Activity. *The Lancet*
397 **315**, 514 (1980).
398 27. R Core Team. *R: A Language and Environment for Statistical Computing*. (R Foundation
399 for Statistical Computing, Vienna, 2022).
400 28. Bates, D., Mächler, M., Bolker, B. & Walker, S. Fitting Linear Mixed-Effects Models Using
401 lme4. *Journal of Statistical Software* **67**, 1–48 (2015).
402 29. Kuznetsova, A., Brockhoff, P. B. & Christensen, R. H. B. lmerTest Package: Tests in Linear
403 Mixed Effects Models. *Journal of Statistical Software* **82**, 1–26 (2017).
404 30. Fox, J. & Weisberg, S. *An R Companion to Applied Regression*. (Sage, Thousand Oaks CA,
405 2019).

406 31. Wickham, H. *Ggplot2: Elegant Graphics for Data Analysis*. (Springer-Verlag, New York,
407 2016).
408 32. Love, M. I., Huber, W. & Anders, S. Moderated estimation of fold change and dispersion
409 for RNA-seq data with DESeq2. *Genome Biol* **15**, 550 (2014).
410 33. Hao, Y. *et al.* Integrated analysis of multimodal single-cell data. *Cell* **184**, 3573-3587.e29
411 (2021).
412

413 **Declarations**

414 *Ethics approval and consent to participate*

415 All research complied with relevant ethical regulations, and usage of human tissue material
416 and transcriptome data was approved by the ethics committee of the Medical Faculty at Kiel
417 University (A156/03, A124/14, TJ301).

418

419 *Consent for publication*

420 Not applicable

421

422 *Availability of data and material*

423 Not applicable. All data was retrieved (see method section).

424

425 *Competing interests*

426 SS reports indirect stock ownership in Gerion Biotech GmbH as well as consulting and
427 personal fees from AbbVie, Allergosan, Amgen, Arena, BMS, Biogen, Celltrion, Celgene, Falk,
428 Ferring, Fresenius, Galapagos/Gilead, HIKMA, I-Mab, Janssen, Lilly, Morphic, MSD, Mylan,
429 Pfizer, Prometheus, Protagonist, Provention Bio, Sandoz/Hexal, Takeda, and Theravance. PR
430 reports stock ownership in Gerion Biotech GmbH and consulting fees from Takeda.

431 All other authors declare no competing interests.

432

433 *Funding*

434 This work was supported by the German Research Foundation (DFG) through the individual
435 grant SO1141/10-1, the Research Unit FOR5042 “miTarget - The Microbiome as a Target in
436 Inflammatory Bowel Diseases” (project P5), the Excellence Cluster EXS2167 “Precision
437 Medicine in Chronic Inflammation” and an intramural grant of the medical faculty of Kiel
438 University (grant no K126408) to FS. The funding bodies had no part or influence on the design
439 of the study and data collection, analysis, or interpretation.

*Authors' contributions*

SW, LJ and FS designed research. SW, JT, LJ and FS performed experiments and analyzed the data. SS, CR, KA and PR provided samples and RNAseq data. SW, JT, LJ and FS prepared the figures. KA, PR, CK and FS obtained funding. SW, JT, LJ and FS co-wrote the manuscript with critical input from all authors. All authors read and approved the final manuscript.

*Acknowledgements*

The authors thank Sabine Kock, Stefanie Baumgarten, Maren Reffelmann, Vivian Wegner, Tanja Klostermeier, Dorina Ölsner, Meike Hansen, Ronja Möhring and Sophie Reiher for excellent technical assistance.

*Authors' information (optional)*

Not applicable

455 **Figures and tables**

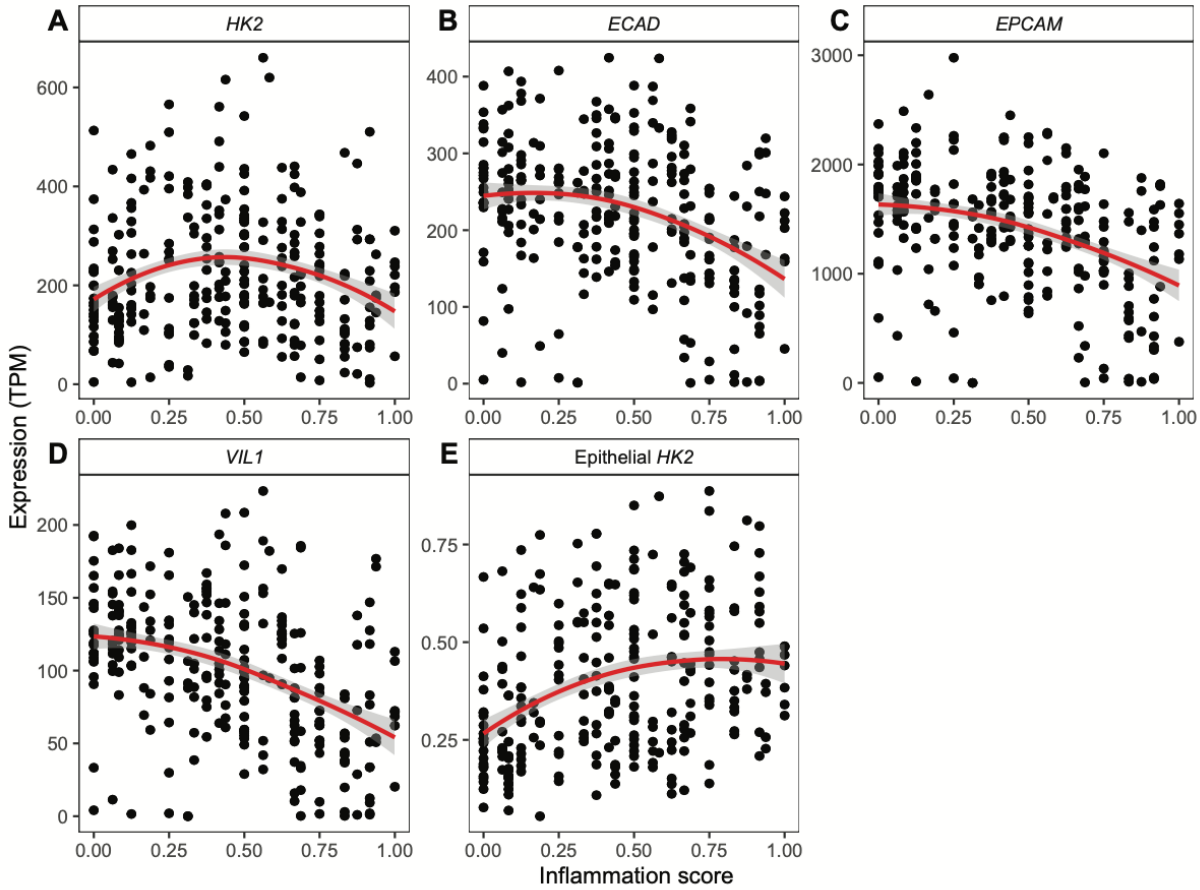


456

457 **Figure 1: Epithelial HK2 expression correlates with inflammation severity. A-D)** Expression
458 (TPM, transcript per million) of *HK2* **(A)** and the epithelial marker genes *ECAD* **(B)***, VIL1* **(C)** and
459 *EPCAM* **(D)** in the intestinal mucosa of patients with various degrees of gut inflammation.
460 Note that at high inflammation scores (>0.4) expression of *HK2* and the epithelial marker
461 genes all decrease indicating epithelial erosion. The inflammation score was calculated as a
462 scaled Harvey-Bradshaw index (Crohn's disease) or Mayo score (ulcerative colitis) to
463 accommodate both disease types. **E)** *HK2* expression increases with inflammation scores after
464 normalization to epithelial marker gene expression. The red lines represent the mean
465 expression trendline. The number in the upper right corner represents the p value for the
466 correlation between gene expression and inflammation score as determined by linear mixed
467 model.

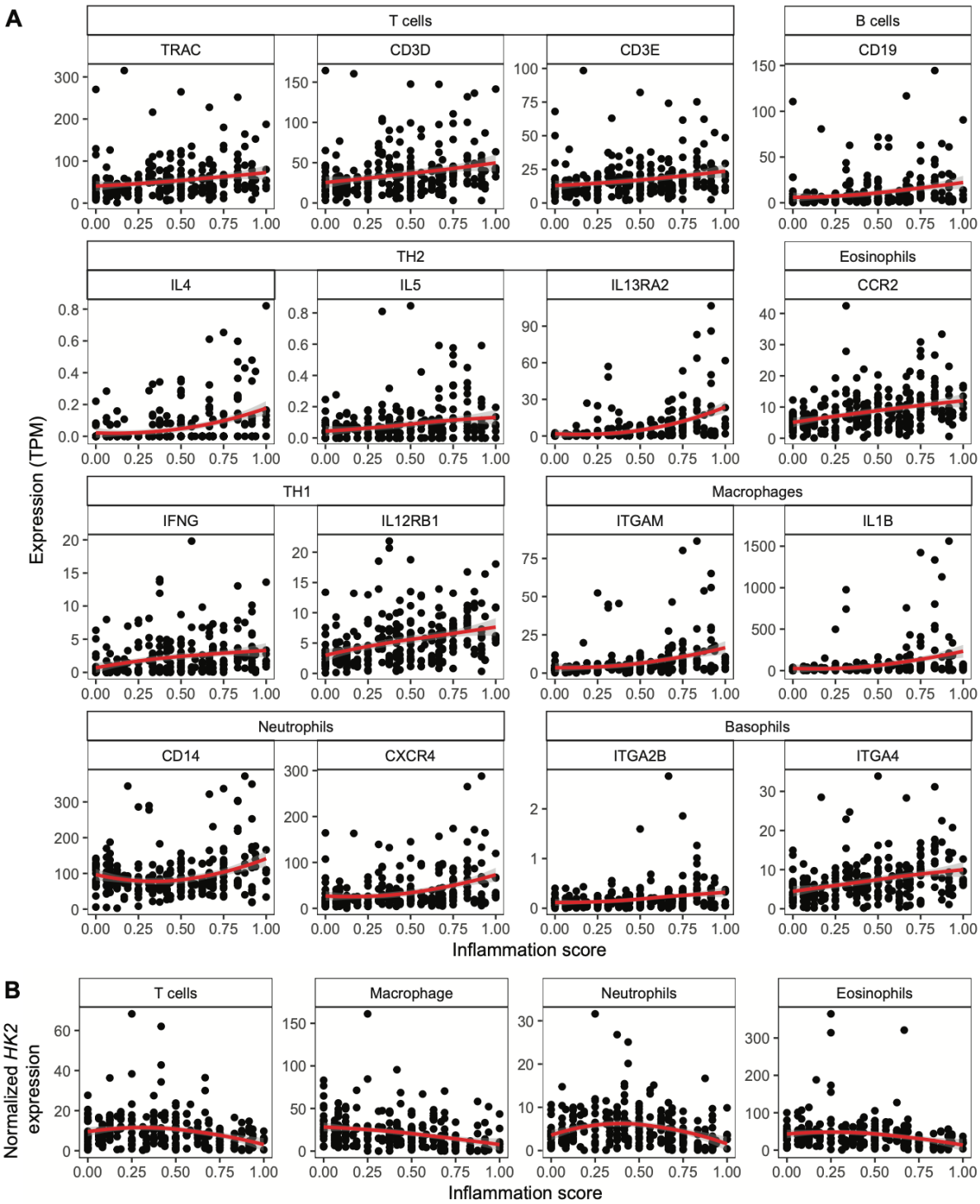


**Figure 2: Expression of candidate immune marker genes increases with inflammation severity.** Expression of selected marker genes, which are characteristic for individual immune cell types, were evaluated in patient biopsies. Expression of virtually all candidate immune marker genes increase with inflammation severity indicating an expansion of immune cells – a known feature of intestinal inflammation.

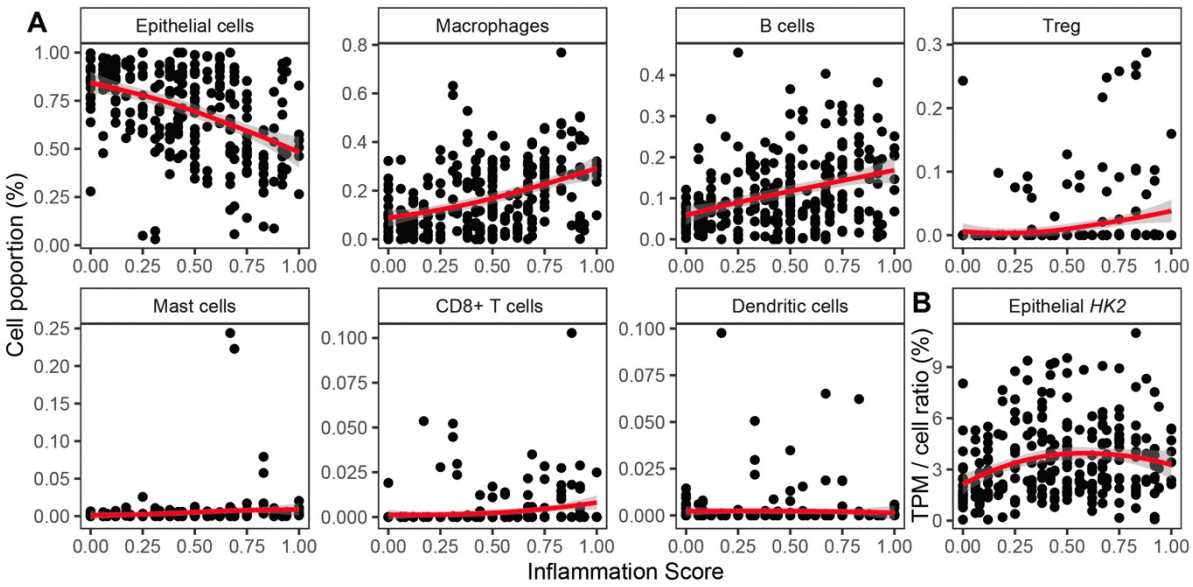


**Figure 3: Deconvolution of mucosal transcriptomes demonstrates cellular remodeling during inflammation. A)** MuSiC cell deconvolution package was used to estimate ratios of the most abundant cell types based on the mucosal patient transcriptomes. Notably, epithelial cell abundance is decreasing with inflammation, whereas abundances of macrophages and B cells, the two most frequent immune cell types that combine for approximately 35 % proportion, are increasing with inflammation severity. Therefore, cell deconvolution supports the candidate gene analyses indicating mucosal cellular remodeling characterized by a reduction of epithelial cells and an expansion of immune cells with increasing inflammation severity. **B)** *HK2* expression increases with inflammation scores after normalization to epithelial cell abundance.

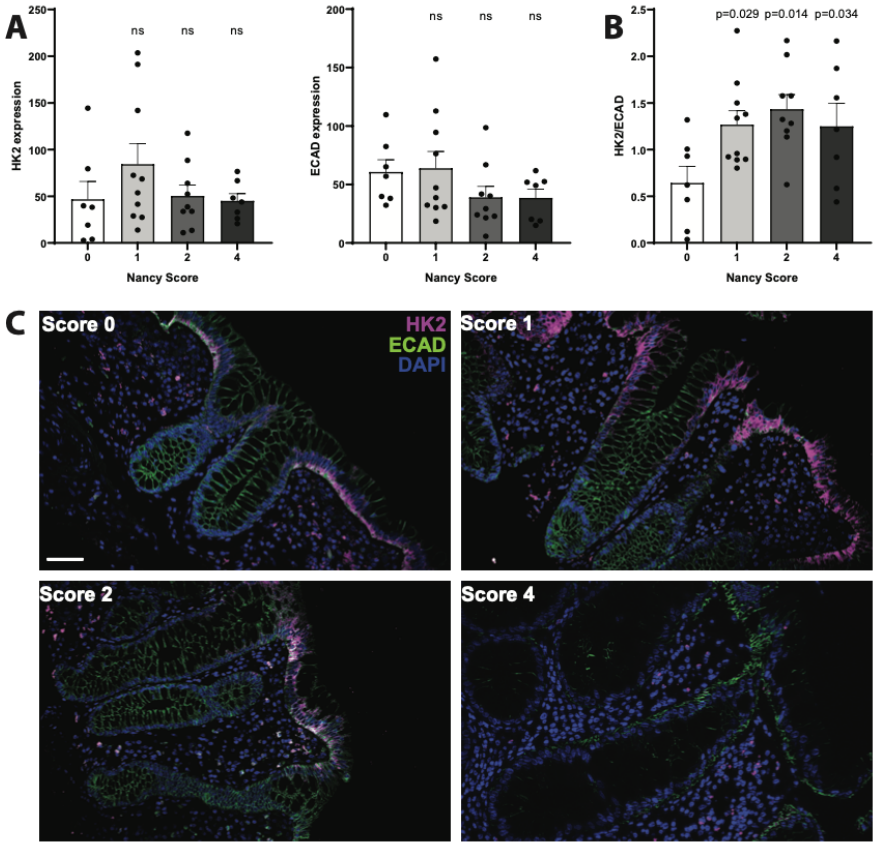


485

486 **Figure 4: Epithelial HK2 protein expression increases with inflammation severity.** Colonic
487 mucosa biopsies of unrelated UC patients were stained for HK2, epithelial cells (ECAD) and
488 nuclei (DAPI). All biopsies were analyzed for classical histological signs of inflammation using
489 the Nancy Score (see method section). **A)** Quantification of HK2 and ECAD signal intensity in
490 apical intestinal epithelium. Note that HK2 and ECAD level decrease with higher Nancy Scores.
491 **B)** HK2 protein expression normalized to ECAD levels. Note that after epithelial normalization
492 HK2 expression increases with inflammation severity, i.e. Nancy Score. Significance testing
493 was performed using one-way ANOVA compared to Score = 0. **C)** Representative images of
494 the multiplex immunofluorescence stainings (HK2, ECAD, DAPI). Scale bar indicates 50 µm. n
495 = 7 – 10 per group. Note that microscopic images were taken from areas with rather intact
496 epithelium for a better visualization of the mucosal structure.

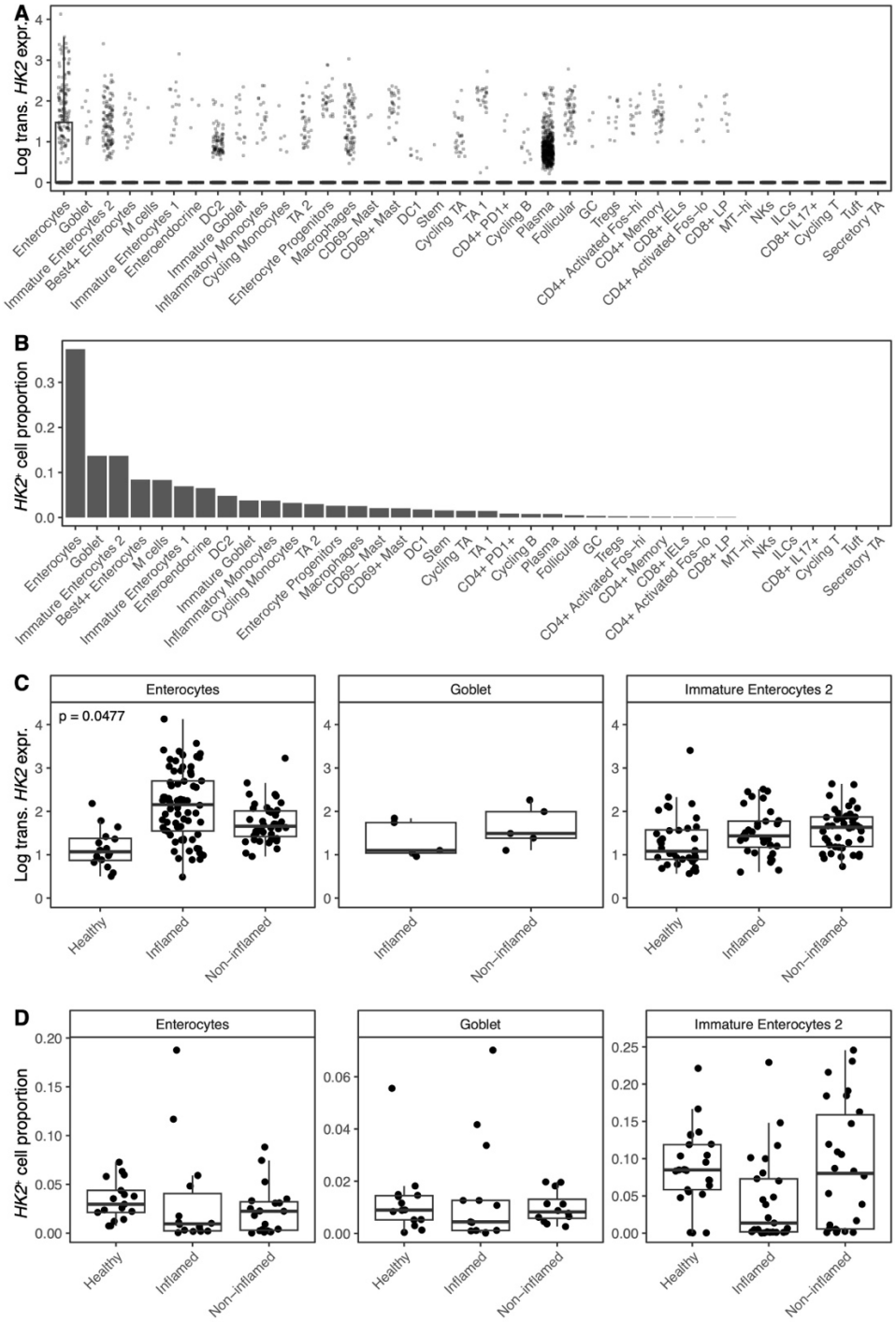


**Figure 5: *HK2* is mainly expressed by mature enterocytes and increased during inflammation.** *HK2* expression was analyzed in published single cell RNA sequencing data derived from mucosal biopsies of UC patients[11]. **A)** *HK2* expression per cell type. **B)** Abundances of cell types expressing *HK2*. **C)** *HK2* expression in mature & immature enterocytes and goblet cells divided into samples from healthy controls, inflamed and non-inflamed mucosa. **D)** Abundances of cell types expressing *HK2* after stratification into disease group.

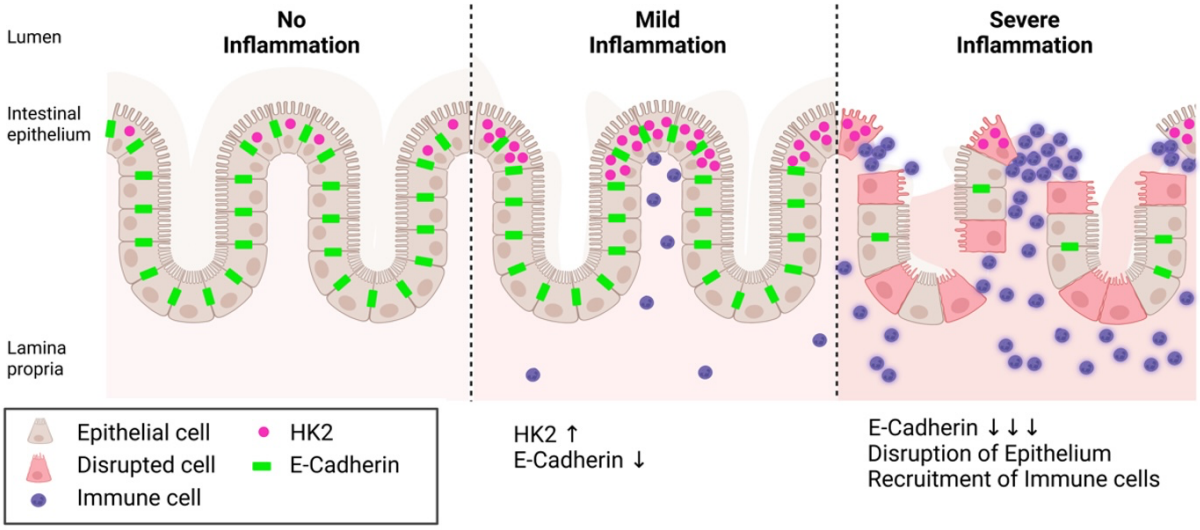


**Figure 6: Model of HK2 expression changes in relation to intestinal inflammation severity.** HK2 is predominantly expressed by apical epithelial cells and HK2 expression in these cells increases with disease severity. However, during the course of inflammation the cellular composition of the mucosa changes. In severely inflamed tissue, the epithelium is disrupted, brush border epithelial cells with high levels of HK2 are shed and lost, whereas immune cells with little to no HK2 expression are recruited. Therefore, overall HK2 expression is reduced in bulk tissue samples under severe inflammation despite local high expression in remaining HK2-positive epithelial cells. Created with BioRender.com

515 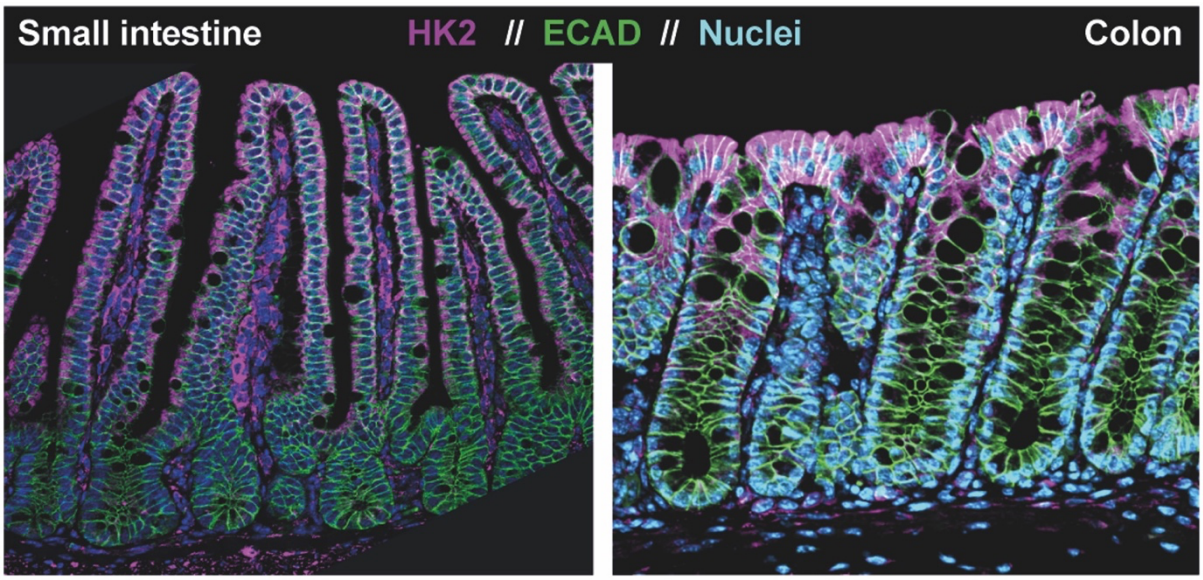


516 **Figure S1: HK2 expression in the intestinal mucosa.** Biopsies from small and large intestine
517 were immuno-stained to localize the HK2 protein in the mucosa. Note that HK2 expression is
518 mainly confined to epithelial cells of the apical mucosa both in the small and large intestine.

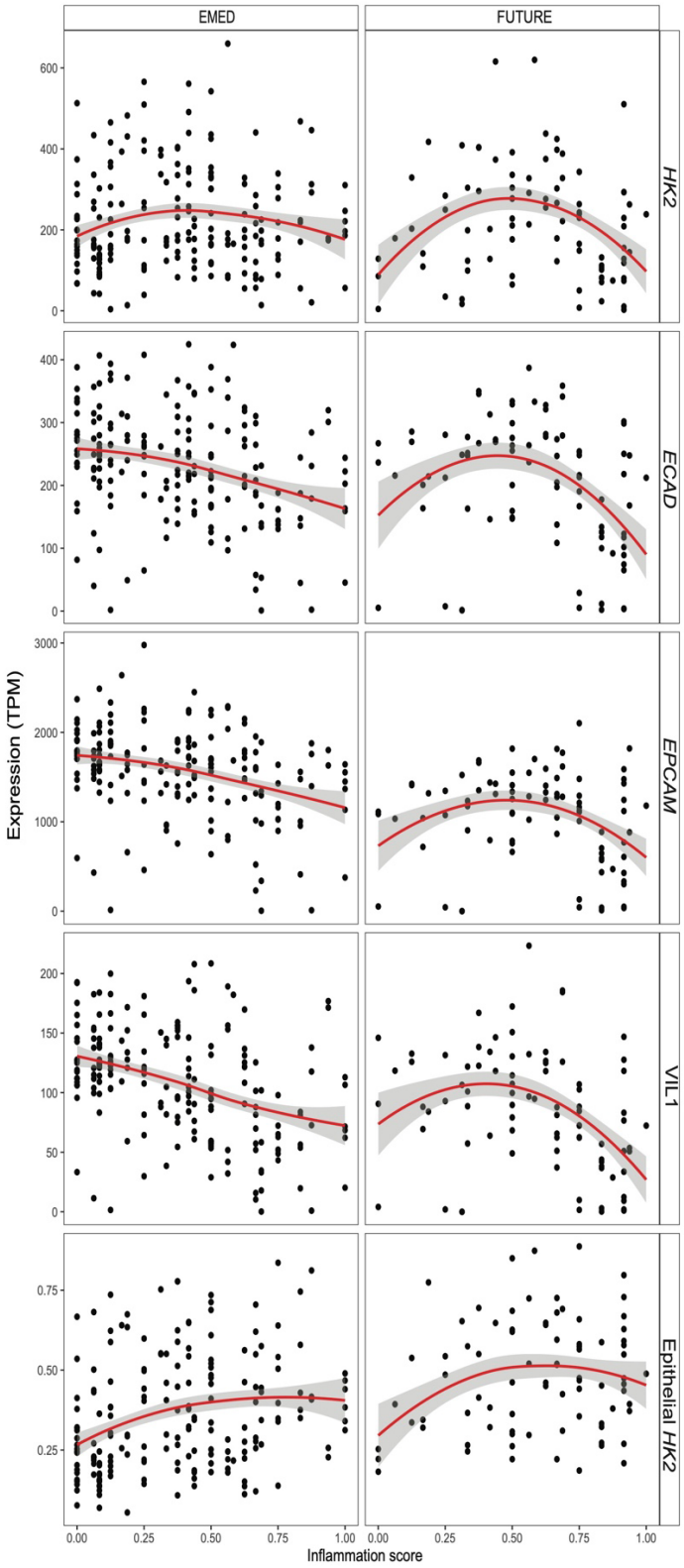


519

520 **Figure S2: Epithelial *HK2* expression correlates with disease severity in both clinical cohorts.**
521 Expression data (TPM, transcript per million) of *HK2* and the epithelial marker genes *ECAD,*
522 *VIL1* and *EPCAM* in the intestinal mucosa of patients with various degrees of gut inflammation
523 split per clinical cohort FUTURE and EMED.

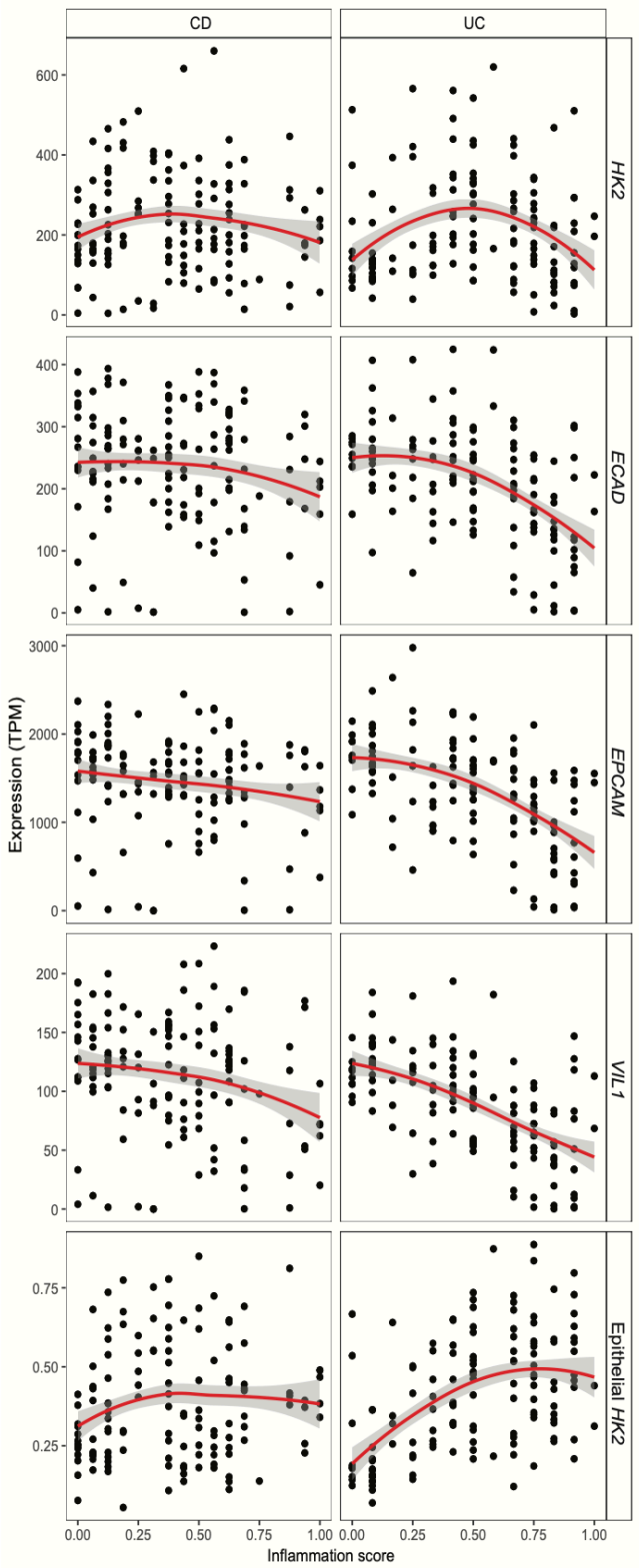


524

525 **Figure S3: Epithelial *HK2* expression correlates with inflammation severity regardless of**
526 **disease subtype.** Expression data (TPM, transcript per million) of *HK2* and the epithelial
527 marker genes *ECAD, VIL1* and *EPCAM* in the intestinal mucosa of patients with various degrees
528 of gut inflammation split per disease subtype CD and UC.

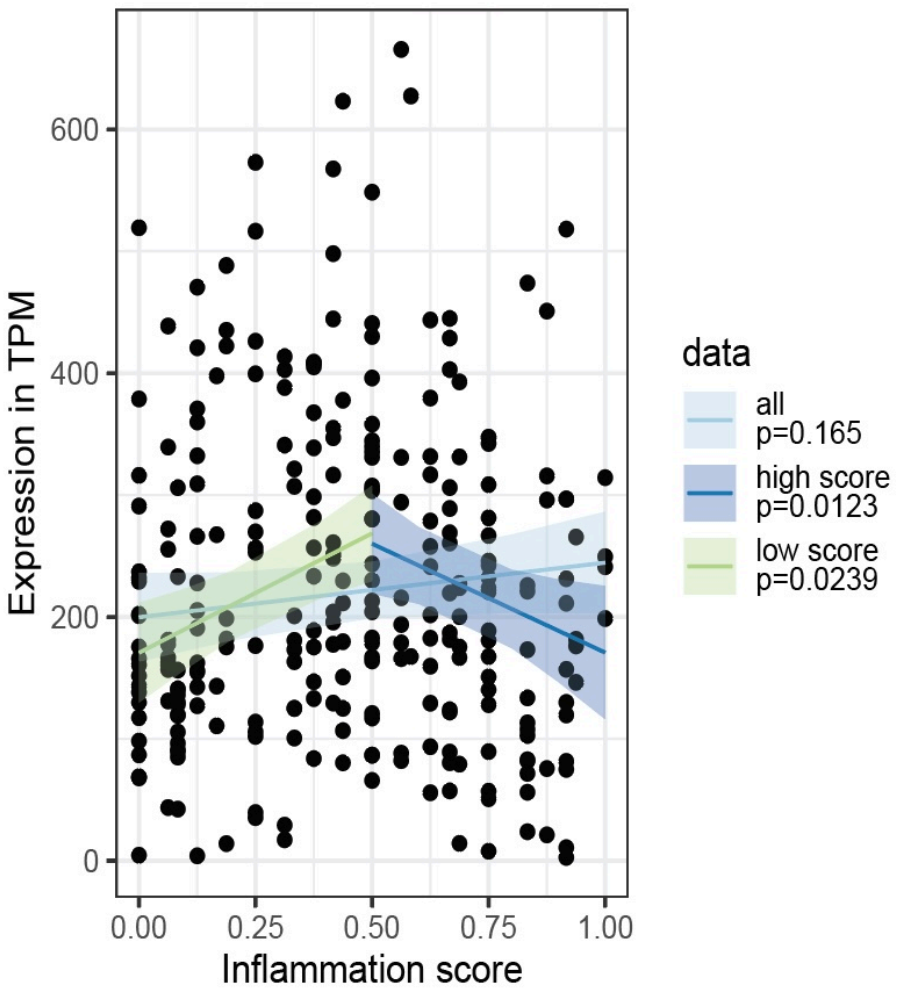


**Figure S4: Correlation analysis for HK2 expression and inflammation score.** Three different linear mixed effect models (PatientID as random factor) were fitted to the data. First, all data points were used to estimate the overall effect of *HK2* expression and inflammation score. Afterwards the data set was split into “low scores” (inflammation score < 0.5), "high scores” (inflammation score >0.5) and fitted models for these data subsets. While the first model showed no significant association between *HK2* expression and inflammation, there is a positive association at “low scores” and a negative association at “high scores” (see also table S1) indicating that *HK2* expression increases with inflammation during lower disease scores and then decreases at higher disease scores.

539 **Table S1: Comparison of linear mixed model statistics for the coefficients explaining HK2**
540 **expression with inflammation scores for models created with all data, low (score <0.5) or**
541 **high (score >0.05) inflammation scores only.**

| | Estimate | Std. Error | DF | t-value | p-value | |
|---|---|---|---|---|---|---|
| **All data** | 44.73 | 32.07 | 179.94 | 1.395 | 0.165 | |
| **Low score** | 195.86 | 59.48 | 154.44 | 3.293 | 0.0123 | ** |
| **High score** | -178.6 | 78 | 114.87 | -2.29 | 0.0239 | * |

542

543 **Table S2: Translation of the HBI and Mayo Score into a general Inflammation Score.** The
544 definitions of the HBI and Mayo scores are listed. The Inflammation Score was calculated by
545 scaling each the HBI and Mayo Score from 0-1 and then merging the scores.

| **HBI** | | |
|---|---|---|
| **Criterium** | **Score** | |
| General well-being | Very well | 0 |
| | Slightly poor | 1 |
| | Poor | 2 |
| | Very poor | 3 |
| | Terrible | 4 |
| Abdominal pain | None | 0 |
| | Mild | 1 |
| | Moderate | 2 |
| | Severe | 3 |
| Abdominal mass | None | 0 |
| | Dubious | 1 |
| | Definite | 2 |
| | Definite with tenderness | 3 |
| Stool frequency | Number of liquid stools | 1 for each lquid stool per day |
| Complications | Arthralgia, Uveitis, Erythema nodosum, Apthous ulcers, Pyoderma gangrenosum, Anal fissure, New fistula, Abscess | 1 point each |

546

| **Mayo Score** | | |
|---|---|---|
| **Criterium** | **Score** | |
| Number of stools per day | Normal for the patient | 0 |
| | 1-2 stools more than normal | 1 |
| | 3-4 stools more than normal | 2 |
| | 5+ stools more than normal | 3 |
| Rectal blood | No blood | 0 |
| | Blood streaks in less the half of evacuations | 1 |
| | Evidence of fresh blood in most of the evacuations | 2 |
| | Bowel movements with fresh blood | 3 |
| Endoscopy | Normal or inactive disease | 0 |
| | Mild disease (erythema, decreased vascular pattern, mild friability) | 1 |
| | Moderate disease (marked erythema, lack of vascular pattern, friability, erosions) | 2 |
| | Severe disease (spontaneous bleeding, ulceration) | 3 |
| Global medical asessment | Normal | 0 |
| | Mild disease | 1 |
| | Moderate disease | 2 |
| | Severe disease | 3 |

547
548

| Calculation of inflammation score | | | | | | | | | | |
|---|---|---|---|---|---|---|---|---|---|---|
| **HBI** | **InfScore** | | **Mayo** | **InfScore** | | **>>>** | | **InfScore** | **HBI** | **Mayo** |
| 0 | 0.00 | | 0 | 0.00 | | merged | | 0.00 | 0 | 0 |
| 1 | 0.06 | | 1 | 0.08 | | | | 0.06 | 1 | |
| 2 | 0.12 | | 2 | 0.17 | | | | 0.08 | | 1 |
| 3 | 0.18 | | 3 | 0.25 | | | | 0.12 | 2 | |
| 4 | 0.24 | | 4 | 0.33 | | | | 0.17 | | 2 |
| 5 | 0.29 | | 5 | 0.42 | | | | 0.18 | 3 | |
| 6 | 0.35 | | 6 | 0.50 | | | | 0.24 | 4 | |
| 7 | 0.41 | | 7 | 0.58 | | | | 0.25 | | 3 |
| 8 | 0.47 | | 8 | 0.67 | | | | 0.29 | 5 | |
| 9 | 0.53 | | 9 | 0.75 | | | | 0.33 | | 4 |
| 10 | 0.59 | | 10 | 0.83 | | | | 0.35 | 6 | |
| 11 | 0.65 | | 11 | 0.92 | | | | 0.41 | 7 | |
| 12 | 0.71 | | 12 | 1.00 | | | | 0.42 | | 5 |
| 13 | 0.76 | | | | | | | 0.47 | 8 | |
| 14 | 0.82 | | | | | | | 0.50 | | 6 |
| 15 | 0.88 | | | | | | | 0.53 | 9 | |
| 16 | 0.94 | | | | | | | 0.58 | | 7 |
| 17 | 1.00 | | | | | | | 0.59 | 10 | |
| | | | | | | | | 0.65 | 11 | |
| | | | | | | | | 0.67 | | 8 |
| | | | | | | | | 0.71 | 12 | |
| | | | | | | | | 0.75 | | 9 |
| | | | | | | | | 0.76 | 13 | |
| | | | | | | | | 0.82 | 14 | |
| | | | | | | | | 0.83 | | 10 |
| | | | | | | | | 0.88 | 15 | |
| | | | | | | | | 0.92 | | 11 |
| | | | | | | | | 0.94 | 16 | |
| | | | | | | | | 1.00 | 17 | 12 |

551 **Table S3: Original and pooled deconvolution cell types.** Originally classified cell types that
552 are ontogenetically related, e.g. Paneth cells, enterocytes, goblet cells and stem cells, were
553 pooled and classified into "epithelial cells" to reduce cell type diversity.

| Original cell type description | Grouped into cell type |
|---|---|
| TA 1 | epis |
| TA 2 | epis |
| Enterocyte Progenitors | epis |
| Immature Goblet | epis |
| Immature Enterocytes 1 | epis |
| Immature Enterocytes 2 | epis |
| Cycling TA | epis |

554